Available online at www.sciencedirect.com
ScienceDirect
Journal of Sound and Vibration 319 (2009) 1107–1120
JOURNAL OF SOUND AND VIBRATION
www.elsevier.com/locate/jsvi

The magneto-elastic subharmonic resonance of current-conducting thin plate in magnetic filed

Hu Yuda*, Li Jing

School of Civil Engineering and Mechanics, Yanshan University, Qinhuangdao 066004, PR China

Received 23 August 2007; received in revised form 14 February 2008; accepted 14 June 2008
Handling Editor L.G. Tham
Available online 13 August 2008

Abstract

Based on Maxwell equations and corresponding electromagnetic constitutive relations, the electrodynamic equations and electromagnetic force expressions of a current-conducting thin plate in electromagnetic field are deduced. Nonlinear magneto-elastic vibration equations of the thin plate are given. In addition, nonlinear subharmonic resonances of the thin plate with two opposite sides simply supported which is under the mechanic live loads and in constant transverse magnetic field are studied. The corresponding vibration differential equation of Duffing type is deduced by the Galerkin method. The method of multiple scales is used to solve the equation, and the frequency-response equation of the system in steady motion under subharmonic responses is obtained, and the stability of solution is analyzed. According to the Liapunov stability theory, the critical conditions of stability are obtained. By the numerical calculation, the curves of resonance amplitude changing with the detuning parameter, the excitation amplitude and the magnetic intensity and corresponding state planes are obtained. The existing regions of nontrivial solutions and the changing law of stable and unstable solutions are analyzed. The time history response plots, the phase charts and the Poincare mapping charts are plotted. And the effect of the magnetic intensity on the system is discussed, and some complex dynamic performances as period-doubling motion and quasi-period motion are analyzed.

1. Introduction

With the fast development of modern science and technology field such as aerospace industry, nuclear industry, magnetic suspension transportation, electromechanical dynamic system, etc. the application of electro-magneto mechanics are more and more extensive. The analysis on magneto-elastic dynamics of structures under the complicated electro-magnetic filed has been more and more focused on. The interaction of many fields such as electromagnetic field, mechanical field, must be considered of, so there are some difficulties during creating models and solving equations. It is still the topic studied in both theoretical and practical.

*Corresponding author.
E-mail address: huyuda03@163.com (H. Yuda).

0022-460X/$ - see front matter
doi:10.1016/j.jsv.2008.06.016

In recent years, the electromagnetic elasticity mechanics developed very quickly. Many researchers from different countries made a lot of theoretical discussion and got some available results. Pao et al. [1,2] create a foundation on the theory of electromagnetic elasticity dynamics by rational mechanic and axiomatization system method. Moon and Eringen [2–4] established some theoretical models of electromagnetic elasticity mechanics of ferromagnetic medium. Papers [5–7] studied the dynamic stability of ferromagnetic elastic beams on theoretical and experimental viewpoints, respectively. Papers [8,9] elaborate about the dynamic and the static stability of a thin plate in magnetic fields and thermal conditions. On the theoretical study of magneto-elastic vibrations of a current-carrying thin plate, Ambarcumian and Moljchenko [10,11] did some creative works and got a lot of available outcomes. Papers [12,13] analyzed the dynamic characteristics of a current-conducting plate under the effect of the electric current and the pulse magnetics, respectively. Paper [14] studied large dynamotor's rotor winding's electro-magnetic elasticity resonance and bifurcation. At present, the focus is on the study of nonlinear vibration, bifurcation and chaotic dynamic of magneto-elastic coupling system. Because many factors affect the system motion and their acting form is complex, there are still many problems need to be further studied.

Based on papers [15,16], this paper further studies the magneto-elastic subharmonic resonance and stability of current-conducting thin plate. The nonlinear vibration Duffing equation and the amplitude–frequency response in the steady motion of a thin plate in the transverse magnetic field are derived. And the stability of solutions is analyzed. At last, by means of calculated examples, the amplitude frequency-response curves, dynamic response charts and Poincare mapping charts are obtained, and the effect of electromagnetic and mechanical parameters on the system are analyzed.

2. The magneto-elastic oscillation equations of current-conducting thin plate

2.1. Electrodynamic equation

Considering the material is a nonpolarized and nonsusceptively good conductor, the specific conductance and magneto-conductivity is same as that in the vacuum. We also can ignore the effect of the displacement current. Therefore, as shown in Fig. 1, in Cartesian coordinate, each electromagnetic measure of internal medium of conductive thin plates should satisfy the Maxwell's electromagnetic equations

$$\nabla \cdot \mathbf{B} = 0, \quad \nabla \cdot \mathbf{D} = 0, \quad \nabla \times \mathbf{E} = -\frac{\partial \mathbf{B}}{\partial t}, \quad \nabla \times \mathbf{H} = \mathbf{J} \tag{1}$$

The electromagnetic constitutive relation is

$$\mathbf{D} = \varepsilon_0 \mathbf{E}, \quad \mathbf{B} = \mu_0 \mathbf{H}, \quad \mathbf{J} = \sigma\left(\mathbf{E} + \frac{\partial \mathbf{u}}{\partial t} \times \mathbf{B}\right) \tag{2}$$

where $\mathbf{B}(B_x,B_y,B_z)$ is the magnetic induction density vector, $\mathbf{H}(H_x,H_y,H_z)$ the magnetic field intensity vector, $\mathbf{J}(J_x,J_y,J_z)$ the current density vector, $\mathbf{D}(D_x,D_y,D_z)$ the electric displacement vector, $\mathbf{E}(E_x,E_y,E_z)$ the electric field intensity vector, $\mathbf{u}(u_x,u_y,u_z)$ the displacement vector of each internal point of the conductor, σ the electric conductance, ε_0 the dielectric constant in the vacuum, μ_0 the permeability in the vacuum, t is time variable, "∇" the Hamilton operator.

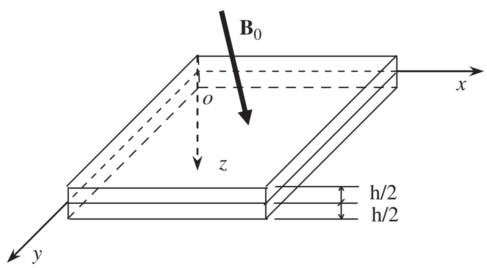

Fig. 1. Current-conducting thin plate in magnetic field.

When the thin plate moves in the external magnetic field, the internal electromagnetic measure can be written as [6]

$$\mathbf{H}(H_x, H_y, H_z) = \mathbf{H}_0(H_{0x}, H_{0y}, H_{0z}) + \mathbf{h}(h_x, h_y, h_z) \tag{3.1}$$

$$\mathbf{B}(B_x, B_y, B_z) = \mathbf{B}_0(B_{0x}, B_{0y}, B_{0z}) + \mathbf{b}(b_x, b_y, b_z) \tag{3.2}$$

$$\mathbf{E}(E_x, E_y, E_z) = \mathbf{e}(e_x, e_y, e_z) \tag{3.3}$$

$$\mathbf{D}(D_x, D_y, D_z) = \mathbf{d}(d_x, d_y, d_z) \tag{3.4}$$

where **h**, **b**, **e**, **d** are electromagnetic measures that excited by perturbation motion.

The displacement of each internal point of the plate can be expressed as

$$u_x(x, y, z, t) = u(x, y, t) + z\theta_x(x, y, t) \tag{4.1}$$

$$u_y(x, y, z, t) = v(x, y, t) + z\theta_y(x, y, t) \tag{4.2}$$

$$u_z(x, y, z, t) = w(x, y, t) \tag{4.3}$$

where u, v, w are the displacement components of the points in middle plane; $\theta_x = -(\partial w/\partial x)$, $\theta_y = -(\partial w/\partial y)$.

Thus, based on the magneto-elastic hypothesis of a thin plate [10], we combine Eqs. (1) and (2), and integrate over the period cycle [$-h/2$, $h/2$], the electrodynamic equations are got as followed:

$$\frac{\partial h_z}{\partial x} + \sigma\left(e_y - \frac{\partial u}{\partial t}B_{0z} + \frac{\partial w}{\partial t}B_{0x}\right) = \frac{h_x^+ - h_x^-}{h} \tag{5}$$

$$\frac{\partial h_z}{\partial y} - \sigma\left(e_x + \frac{\partial v}{\partial t}B_{0z} - \frac{\partial w}{\partial t}B_{0y}\right) = \frac{h_y^+ - h_y^-}{h} \tag{6}$$

$$\frac{\partial e_y}{\partial x} - \frac{\partial e_x}{\partial y} + \mu_0\frac{\partial h_z}{\partial t} = 0 \tag{7}$$

where h_x^+ $(x,y,h/2,t)$, h_x^- $(x,y,-h/2,t)$ are the perturbation magnetic induction density of the surface and h is the thickness of plate.

2.2. The expression of electromagnetic force

The expression of the Lorenz force in the magnetic field produced by amoeboid movement body is

$$\mathbf{f}(f_x, f_y, f_z) = \mathbf{J} \times \mathbf{B} \tag{8}$$

Using the third equation of Eq. (2), and integrating along the thickness, the expression of electromagnetic force and moment in a unit area of thin plate is obtained:

$$F_x = \sigma h B_{0z}\left(e_y + B_{0x}\frac{\partial w}{\partial t} - B_{0z}\frac{\partial u}{\partial t}\right) \tag{9}$$

$$F_y = \sigma h B_{0z}\left(-e_x + B_{0y}\frac{\partial w}{\partial t} - B_{0z}\frac{\partial v}{\partial t}\right) \tag{10}$$

$$F_z = \sigma h B_{0y}\left(e_x - B_{0y}\frac{\partial w}{\partial t} + B_{0z}\frac{\partial v}{\partial t}\right) - \sigma h B_{0x}\left(e_y + B_{0x}\frac{\partial w}{\partial t} - B_{0z}\frac{\partial u}{\partial t}\right) \tag{11}$$

$$m_x = \frac{\sigma h^3}{12}B_{0z}^2\frac{\partial^2 w}{\partial t\,\partial x} \tag{12}$$

$$m_y = \frac{\sigma h^3}{12}B_{0z}^2\frac{\partial^2 w}{\partial t\,\partial y} \tag{13}$$

2.3. The nonlinear magneto-elasticity vibration equation

We consider the interaction of mechanic field and electromagnetic field. On the basis of the basic hypothesis of thin plates and the principle of virtual work, we can get the nonlinear magneto-elasticity vibration equations of the plate under the condition of electromagnetic field [15]

$$\frac{\partial N_x}{\partial x}+\frac{\partial N_{xy}}{\partial y}+F_x+P_x=\rho h\frac{\partial^2 u}{\partial t^2} \tag{14}$$

$$\frac{\partial N_y}{\partial y}+\frac{\partial N_{xy}}{\partial x}+F_y+P_y=\rho h\frac{\partial^2 v}{\partial t^2} \tag{15}$$

$$\frac{\partial^2 M_x}{\partial x^2}+\frac{\partial^2 M_y}{\partial y^2}+2\frac{\partial^2 M_{xy}}{\partial x\,\partial y}+\frac{\partial}{\partial x}\left(N_x\frac{\partial w}{\partial x}+N_{xy}\frac{\partial w}{\partial y}\right)+\frac{\partial}{\partial y}\left(N_y\frac{\partial w}{\partial y}+N_{xy}\frac{\partial w}{\partial x}\right)+\frac{\partial m_x}{\partial x}+\frac{\partial m_y}{\partial y}+F_z+P_z =\rho h\frac{\partial^2 w}{\partial t^2} \tag{16}$$

where N_x, N_y, N_{xy} are in-plane efforts; M_x, M_y, M_{xy} are bending moments, P_x, P_y, P_z are mechanical load and ρ is density of the material.

Combining all equations we have got, and considering corresponding constitutive and geometrical equations, then we got the nonlinear electromagnetic elasticity vibration equations which describe current-conducting thin plate.

3. The subharmonic vibration of current-conducting thin plate in transverse magnetic filed

3.1. Nonlinear magneto-elastic vibration equations

Discussing the current-conducting metal thin plate under the mechanic dynamic load $P_z=p_0\sin\Omega t$ (p_0 is the amplitude of the live force, Ω is the frequency) in the constant transverse magnetic field $\mathbf{B}_0(0,0,B_{0z})$. Studying the magneto-elastic vibration of rectangular beam–plate with two opposite sides simply supported ($x=0,l$) and other two sides free. Based on the magneto-elasticity vibration equation and the expression of electromagnetic force, ignore the effect of inertia force in middle surface, the nonlinear magneto-elastic vibration equations of beam–plate in transverse field leads to the following equation:

$$D_M\frac{\partial^4 w}{\partial x^4}+\rho h\frac{\partial^2 w}{\partial t^2}-\frac{3}{2}D_N\left(\frac{\partial w}{\partial x}\right)^2\frac{\partial^2 w}{\partial x^2}-\frac{\sigma h^3 B_{0z}}{12}\frac{\partial^3 w}{\partial t\,\partial x^2}-P_z=0 \tag{17}$$

Here, $D_N=Eh/(1-v^2)$ is the tensile strength, $D_M=Eh^3/12(1-v^2)$ is the flexural strength, E the Young's modulus and v the Poisson ratio.

The solution of Eq. (17) in first mode expansion form, which satisfies the boundary condition, is given as follows:

$$w(x,t)=\Phi(t)\sin\frac{\pi x}{l} \tag{18}$$

Substituting Eq. (18) into Eq. (17), using the Galerkin method to integrate the above equations, the nondimensional Duffing equation with damping item is derived:

$$\ddot{q}+q+\eta_{01}\dot{q}+\eta_{02}q^3=\eta_{03}\cos\Omega_0\tau \tag{19}$$

where

$$\eta_{01}=\frac{\sigma h^2 B_{0z}^2}{12\rho\omega_n}\left(\frac{\pi}{l}\right)^2,\quad \eta_{02}=\frac{3D_N h}{8\rho\omega_n^2}\left(\frac{\pi}{l}\right)^4,\quad \eta_3=\frac{4p_0}{\pi\rho h^2\omega_n^2},\quad \omega_n=\sqrt{\frac{D_M}{\rho h}}\left(\frac{\pi}{l}\right)^2$$

nondimensional term $\tau=\omega_n t$, $q=\Phi/h$, $\Omega_0=\Omega/\omega_n$, $\dot{q}$ and $\ddot{q}$ are corresponding the first and second derivative of q with respect to τ.

3.2. The solving method of subharmonic resonance

Considering the hard excitation to analyze the subharmonic resonance ($\Omega_0 \approx 3$) of the thin plate. Take Eq. (19) as

$$\ddot{q} + q = -\varepsilon\eta_1\dot{q} - \varepsilon\eta_2 q^3 + \eta_3 \cos \Omega_0\tau \tag{20}$$

where $\eta_1 = \eta_{01}/\varepsilon$, $\eta_2 = \eta_{02}/\varepsilon$, $\eta_3 = \eta_{03}$ and ε is the lead-in parameter.

Solving the above equation by the method of multiple scales [17,18] and expressing the approximate solution as

$$q(\tau, \varepsilon) = q_0(T_0, T_1) + \varepsilon q_1(T_0, T_1) + \cdots \tag{21}$$

Here, new independent variable $T_0 = \tau$, $T_1 = \varepsilon\tau$.

Substituting Eq. (21) into Eq. (20) and equate coefficients of like powers of ε at each side of the equation. We can obtain

$$D_0^2 q_0 + q_0 = \eta_3 \cos \Omega_0 T_0 \tag{22}$$

$$D_0^2 q_1 + q_1 = -2D_0D_1q_0 - \eta_1 D_0 q_0 - \eta_2 q_0^3 \tag{23}$$

where $D_0 = \partial/\partial T_0$, $D_1 = \partial/\partial T_1$, $D_0^2 = \partial^2/\partial T_0^2$.

The general solution of Eq. (22) can be written as

$$q_0 = A(T_1)\exp(\mathrm{i}T_0) + \Lambda \exp(\mathrm{i}\Omega_0 T_0) + \mathrm{cc} \tag{24}$$

where $\Lambda = \eta_3(1-\Omega_0^2)^{-1}/2$, $\mathrm{i}^2 = -1$, cc expresses conjugate complex items of the front items.

Then substitute Eq. (24) into Eq. (23), we can get

$$\begin{aligned} D_0^2 q_1 + q_1 = & -(2\mathrm{i}A' + \mathrm{i}\eta_1 A + 6\eta_2\Lambda^2 A + 3\eta_2 A^2\bar{A})\exp(\mathrm{i}T_0) - \Lambda(\mathrm{i}\eta_1\Omega_0 + 3\eta_2\Lambda^2 \\ & + 6\eta_2 A\bar{A})\exp(\mathrm{i}\Omega_0 T_0) - \eta_2\{A^3 \exp(3\mathrm{i}T_0) + \Lambda^3 \exp(3\mathrm{i}\Omega_0 T_0) + 3A^2\Lambda \exp[\mathrm{i}(2+\Omega_0)T_0] \\ & + 3\bar{A}^2\Lambda \exp[\mathrm{i}(\Omega_0 - 2)T_0] + 3A\Lambda^2 \exp[\mathrm{i}(1+2\Omega_0)T_0] + 3A\Lambda^2 \exp[\mathrm{i}(1-2\Omega_0)T_0]\} + \mathrm{cc} \end{aligned} \tag{25}$$

where the apostrophe expresses the first derivative about T_1, $\bar{A}$ express the conjugate complex of A.

In order to solve the equation, we lead the detuning parameter δ, and let $\Omega_0 = 3 + \varepsilon\delta$. To eliminate the secular term, we put

$$\mathrm{i}(2A' + \eta_1 A) + 6\eta_2 A\Lambda^2 + 3\eta_2 A^2\bar{A} + 3\eta_2\bar{A}^2\Lambda \exp(\mathrm{i}\delta T_1) = 0 \tag{26}$$

Letting $A(T_1) = (1/2)a(T_1)\exp[\mathrm{i}\beta(T_1)]$ in Eq. (26) and separating real and imaginary parts, we obtain

$$a' = -\frac{\eta_1}{2}a - \frac{3}{4}\eta_2\Lambda a^2 \sin\gamma \quad (g = \delta T_1 - 3\beta) \tag{27.1}$$

$$a\gamma' = (\delta - 9\eta_2\Lambda^2)a - \frac{9}{8}\eta_2 a^3 - \frac{9}{4}\eta_2\Lambda a^2 \cos\gamma \tag{27.2}$$

Under the condition of steady motion, let $a' = \gamma' = 0$, then based on the above two equations and eliminate γ, we can finally obtain the amplitude frequency-response equation as

$$\tfrac{9}{4}\eta_1^2 + (\delta - 9\eta_2\Lambda^2 - \tfrac{9}{8}\eta_2 a^2)^2 = \tfrac{81}{16}\eta_2^2\Lambda^2 a^2 \tag{28}$$

The solution of Eq. (28) can also be expressed as

$$a^2 = k_1 \pm (k_1^2 - k_2)^{1/2} \tag{29}$$

where

$$k_1 = \frac{8\delta}{9\eta_2} - 6\Lambda^2, \quad k_2 = \frac{64}{81\eta_2^2}\left[\frac{9\eta_1^2}{4} + (\delta - 9\eta_2\Lambda^2)^2\right]$$

Because k_2 is the positive value, the nontrivial solution can only exist in the condition of $k_1 > 0$ and $k_1^2 > k_2$.

3.3. The analysis of stability

When we analyze the stability of equilibrium solution under tiny disturbance, we can use following assumption:

$$a = a_0 + a_1, \quad \gamma = \gamma_0 + \gamma_1 \tag{30}$$

where a_0, γ_0 are equilibrium solutions of steady motion, a_1, γ_1 are tiny disturbance terms.

Substituting Eq. (30) into Eq. (27), and expanding for small a_1 and γ_1, noting that a_0 and γ_0 satisfy Eq. (27), and keeping linear terms in a_1 and γ_1, we obtain

$$a_1' = \frac{\eta_1}{2} a_1 - \left(\frac{3\eta_2}{4} \Lambda a_0^2 \cos \gamma_0\right)\gamma_1 \tag{31.1}$$

$$\gamma_1' = -\frac{9\eta_2}{4}(a_0 + \Lambda \cos \gamma_0) a_1 - \frac{3\eta_1}{2}\gamma_1 \tag{31.2}$$

Based on the Lyapunov stability approximation theory, the stability of equilibrium solution of Eq. (27) depends on the eigenvalue of the coefficient matrix on the right-hand sides of Eq. (31). Through the Jacobi matrix of Eq. (31), we can obtain the following eigenvalue equation:

$$\begin{vmatrix} \frac{\eta_1}{2} - \lambda & -\frac{3\eta_2}{4}\Lambda a_0^2 \cos \gamma_0 \\ -\frac{9\eta_2}{4}(a_0 + \Lambda \cos \gamma_0) & -\frac{3\eta_1}{2} - \lambda \end{vmatrix} = 0 \tag{32}$$

If considering the condition that a_0 and γ_0 are the equilibrium solutions of Eq. (27), expanding the above determinant yields

$$\lambda_2 + c_1\lambda + c_2 = 0 \tag{33}$$

where $c_1 = \eta_1$

$$\begin{aligned} c_2 &= -3\left(\frac{3\eta_2}{4}\right)^2 \Lambda a_0^2 (a_0 + \Lambda \cos \gamma_0)\cos \gamma_0 - \frac{3}{4}\eta_1^2 \\ &= \frac{3}{2}\left(\frac{3\eta_2 a_0}{4}\right)^2 (a_0^2 - k_1) \end{aligned}$$

here the expression of k_1 is the same as Eq. (29).

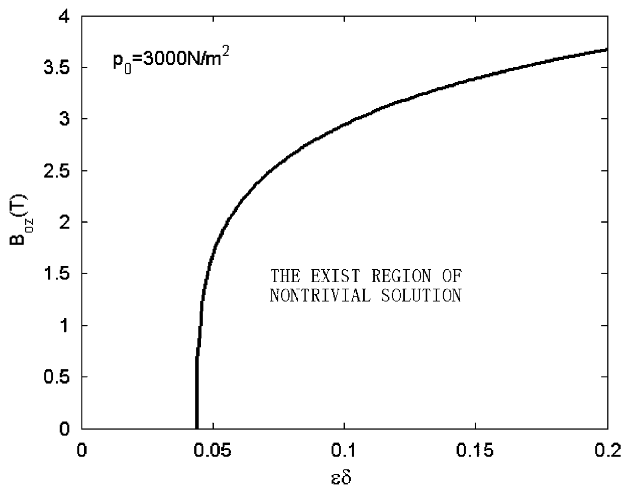

Fig. 2. The existing region of subharmonic resonance (B_{0z}~$\varepsilon\delta$).

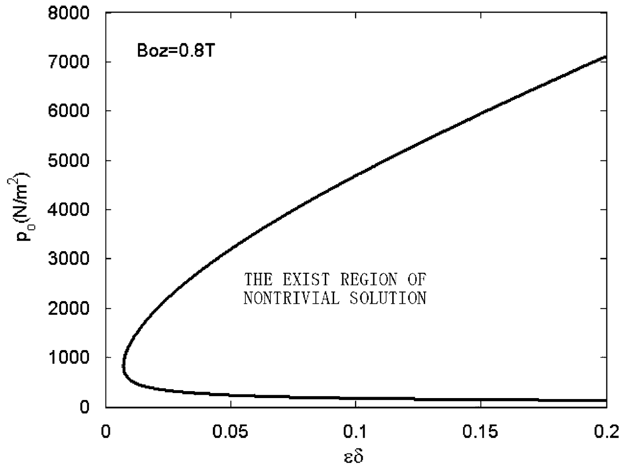

Fig. 3. The existing region of subharmonic resonance ($p_0 \sim \varepsilon\delta$).

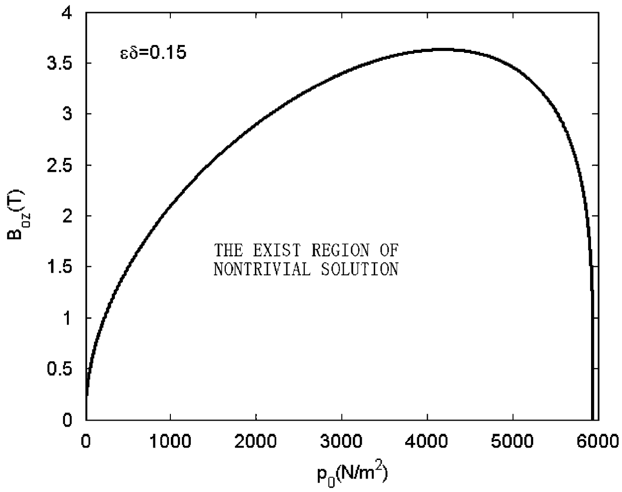

Fig. 4. The existing region of subharmonic resonance ($B_{0z} \sim p_0$).

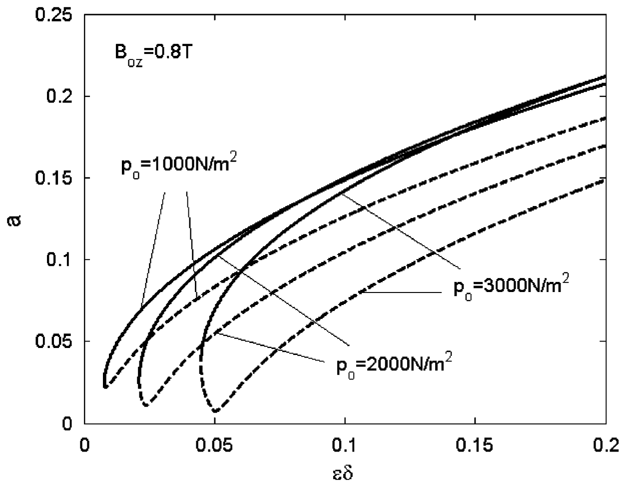

Fig. 5. The amplitude–detuning parameter curve.

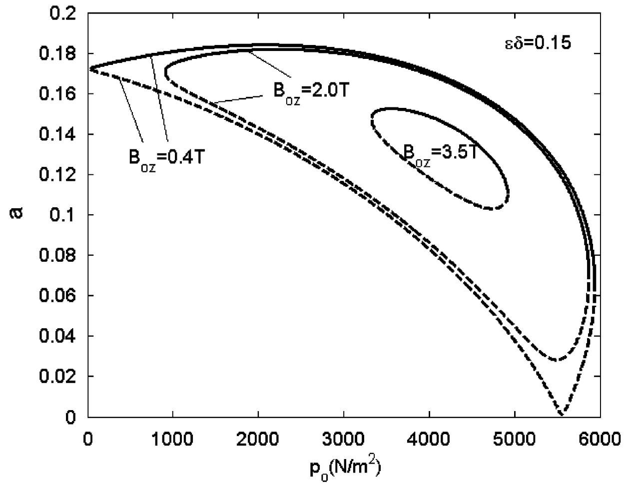

Fig. 6. The amplitude–excitation amplitude curve.

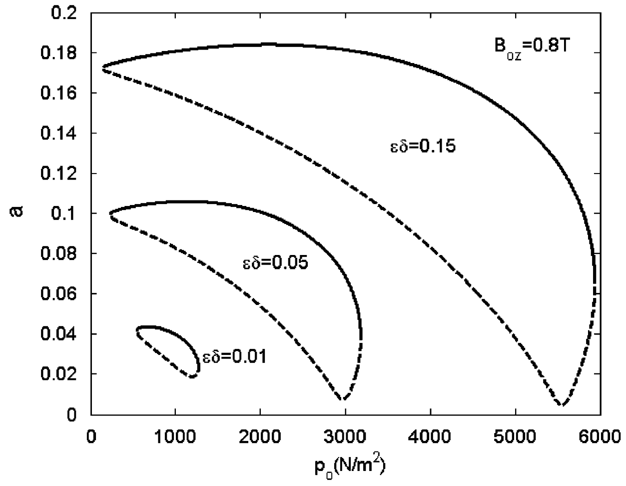

Fig. 7. The amplitude–excitation amplitude curve.

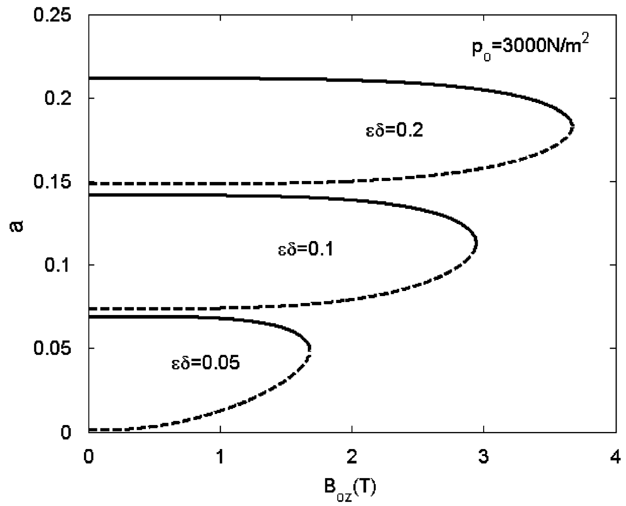

Fig. 8. The amplitude–magnetic density curve.

Then according to Routh–Hurwitz criterion, we can get the necessary and sufficient condition which makes the equilibrium solution stable under the condition of $\eta_1 > 0$ as

$$a_0^2 > k_1 \tag{34}$$

4. The analysis of numerical results

Considering the aluminum thin plate, the main parameters are the electric conductivity $\sigma = 3.63 \times 10^7\,\Omega/\mathrm{m}$, the density $\rho = 2670\,\mathrm{kg/m^3}$, the Poisson parameter $v = 0.34$, Young's modulus $E = 71\,\mathrm{GPa}$, the thickness $h = 4\,\mathrm{mm}$ and the dimension $l = 0.4\,\mathrm{m}$.

Figs. 2–4 correspondingly give the condition of existence of solutions in subharmonic resonance. Through the evolution law of curves in Figs. 2 and 3, we can see that if given the relevant excitation amplitude value or magnetic intensity the nontrivial solution does not exist when $\varepsilon\delta = 0$. The subharmonic resonance of the system can only be excited when the detuning parameter reaches a certain value. Fig. 4 indicates that when we

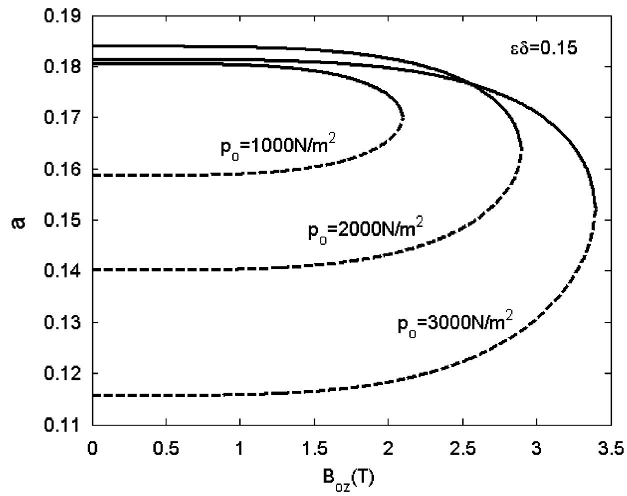

Fig. 9. The amplitude–magnetic density curve.

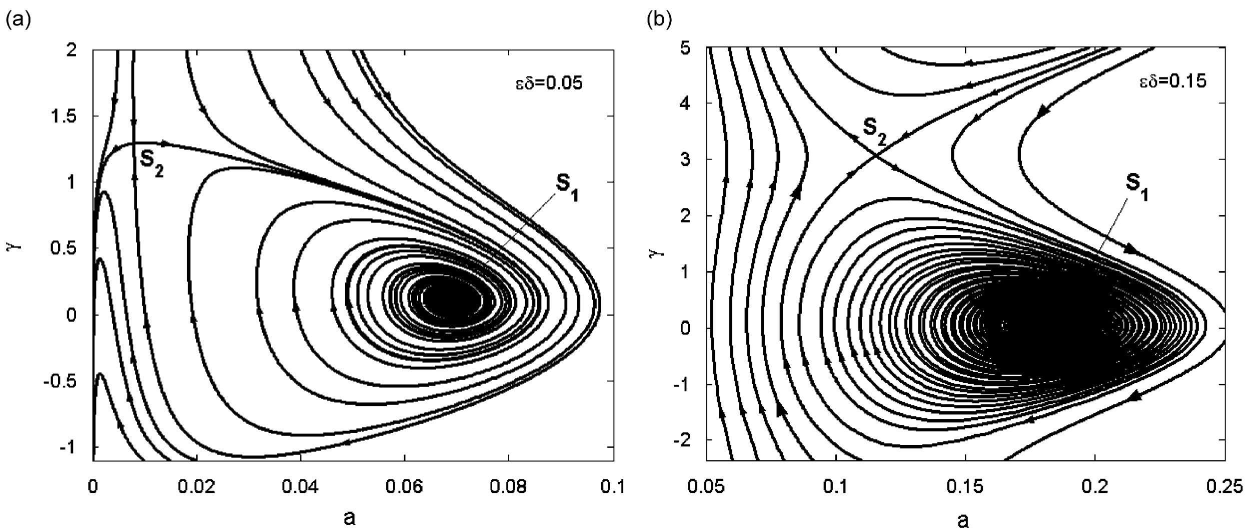

Fig. 10. The phase trajectory chart of state plane ($p_0 = 3000\,\mathrm{N/m^2}$, $B_{0z} = 0.8\,\mathrm{T}$): (a) $\varepsilon\delta = 0.05$, (b) $\varepsilon\delta = 0.15$.

choose properly detuning parameter and only the excitation amplitude value in a specific range the nontrivial solution can exist. But when the magnetic intensity reaches some values leading the nontrivial solution not to exist, the subharmonic resonance is not excited.

Figs. 5–9 are the characteristic curves that resonance amplitude varies with detuning parameter, excitation amplitude and magnetic induction intensity (the real line represents stable solution and the dashed represents unstable solution). From Fig. 5, we can know that with the increase of detuning parameter the resonance first be excited at $p_0 = 1000\,\mathrm{N/m^2}$, then at $p_0 = 2000\,\mathrm{N/m^2}$, last at $p_0 = 3000\,\mathrm{N/m^2}$. When the detuning parameter reaches a certain value, the change of excitation amplitude affects amplitude a little. Fig. 6 indicates that when the detuning parameter is at a definite value, with the increase of magnetic intensity, the range of excitation amplitude which can excite the resonance is narrower. Fig. 7 indicates that when the magnetic intensity is at a definite value, with the increase of detuning parameter, the range of excitation amplitude which can excite resonance is wider but narrower in the opposite case. Fig. 8 indicates that when the excitation amplitude is at a definite value, with the increase of detuning parameter, the range of magnetic intensity which can excite resonance is wider but narrower in the opposite case. The resonance amplitude increases with the increase of detuning parameter. From Fig. 9, we can see that when the detuning parameter at a certain value and the magnetic intensity in some certain range, the change of excitation amplitude has a little effect on resonance

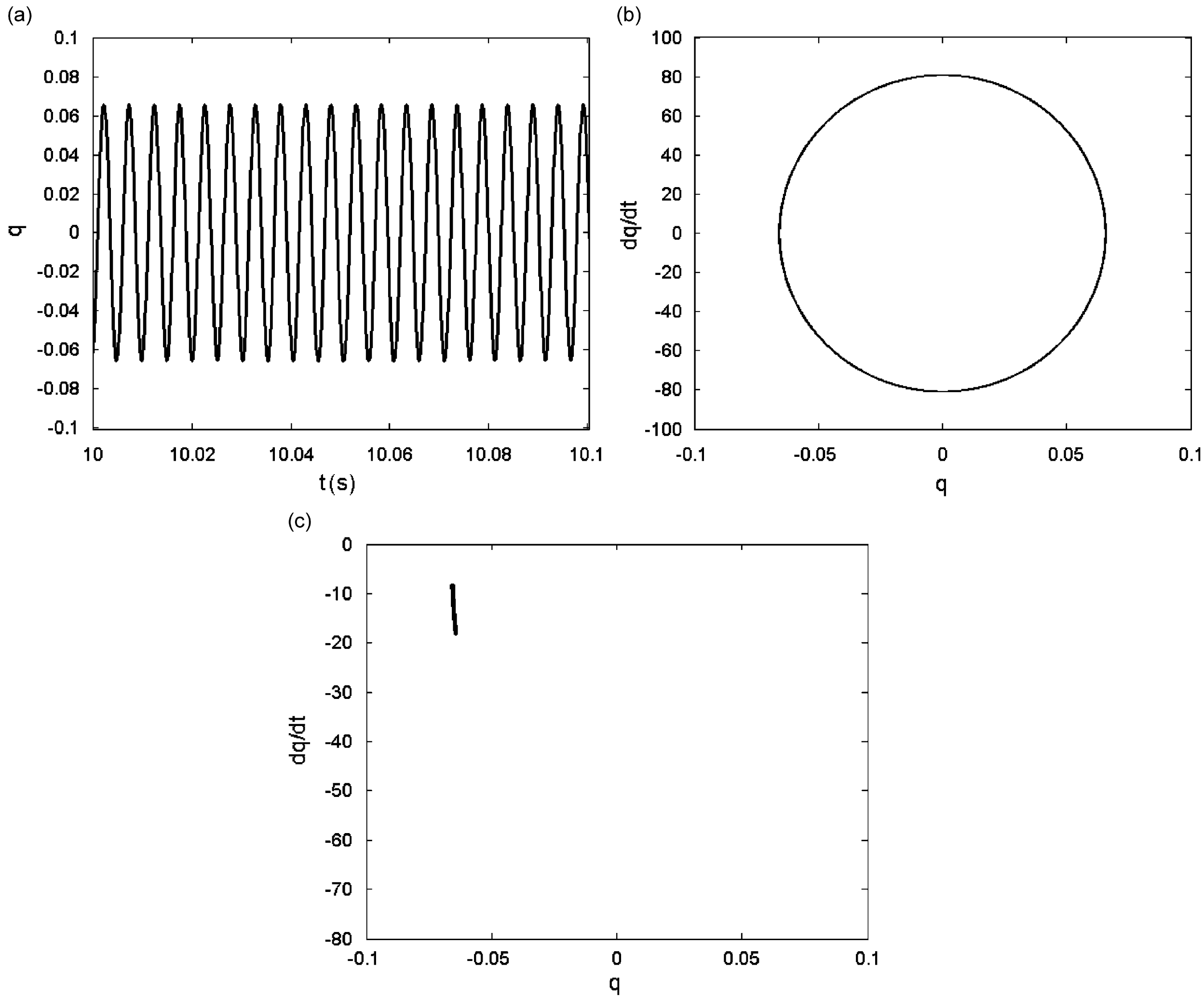

Fig. 11. The vibration characteristic plot ($B_{0z} = 3.5\,\mathrm{T}$): (a) The time history response plot. (b) The phase chart. (c) Poincare mapping chart.

amplitude. But when $B_{0z} = 2.55\,\text{T}$, the two lines which corresponding to $p_0 = 2000$ and $3000\,\text{N/m}^2$ intersect which means that they have the same amplitude.

Fig. 10 is the phase trajectory chart of moving phase plane. S_1 is the stable focus, S_2 the saddle and the trend of orbital depends on initial conditions. From the specific position of the focus and the saddle, we can see that when $\varepsilon\delta = 0.05$ the stable solution is $a = 0.069$ and the unstable solution is $a = 0.008$; when $\varepsilon\delta = 0.15$ the stable solution is $a = 0.182$ and the unstable solution is $a = 0.116$. These numeric values are anastomose with the above amplitude characteristic curves.

In order to analyze the complex dynamic character of system further, in a given excitation amplitude value ($p_0 = 3000\,\text{N/m}^2$) and detuning parameter ($\varepsilon\delta = 0.15$), by changing magnetic intensity value, we obtain the corresponding time history response plot, the phase chart and the Poincare mapping chart (Figs. 11–14). From these figures, we can know that when $B_{0z} = 3.5\,\text{T}$ (Fig. 11) the subharmonic resonance is not excited and the system expresses stable single-frequency periodic motion excited by external excitation. The phase chart is a closed circle, the Poincare mapping chart expresses a small clusters of points set. When $B_{0z} = 2.0\,\text{T}$ (Fig. 12) the subharmonic resonance is excited. The system expresses the classical stable period-doubling motion. The phase chart is the closed curve twice intersected by three circles. The Poincare mapping chart expresses three separated clusters of point sets. This is the typical form of the stable period-doubling motion. When $B_{0z} = 0.4\,\text{T}$ (Fig. 13) system expresses the combinative motion of quasi-period motion and period-doubling

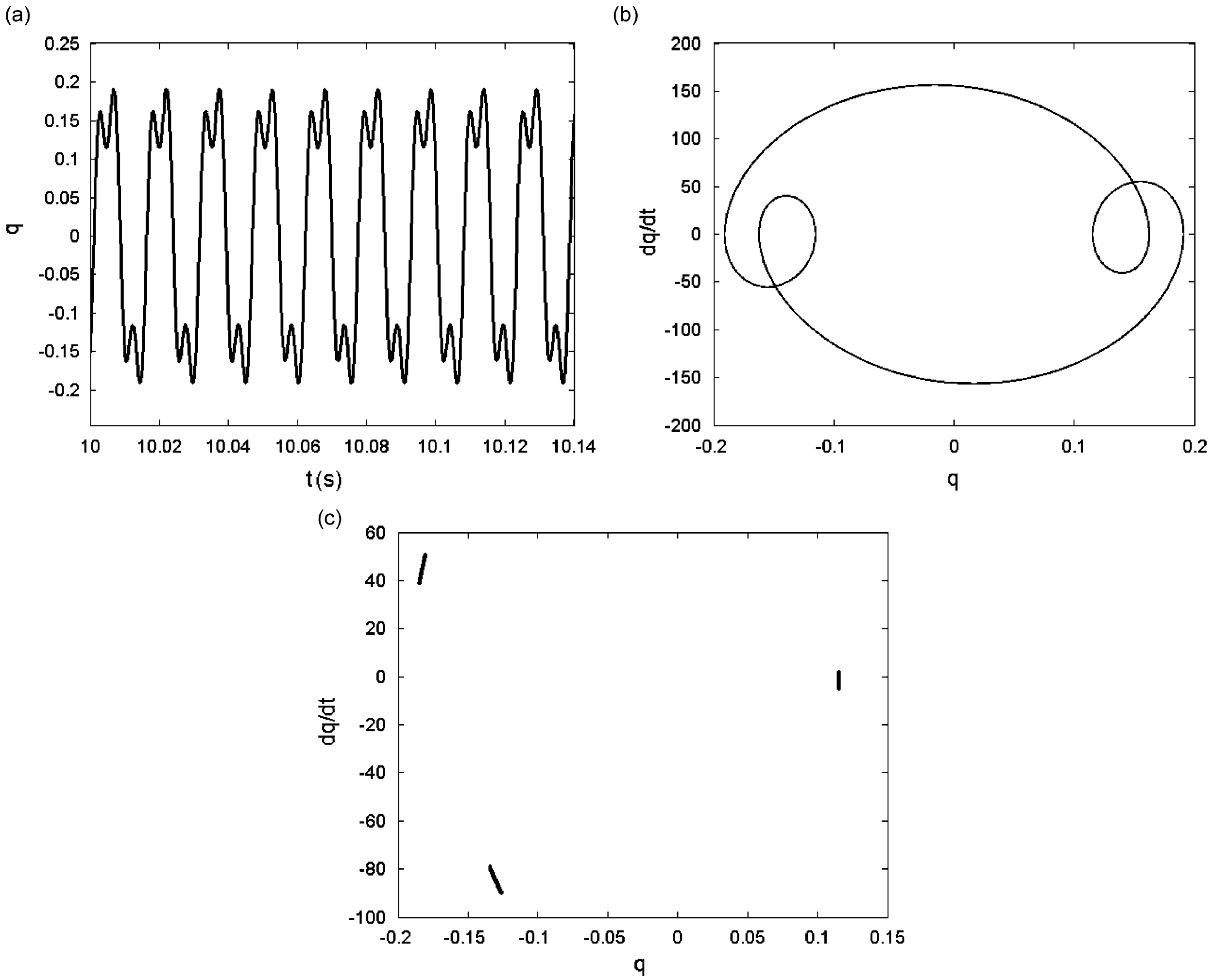

Fig. 12. The vibration characteristic plot ($B_{0z} = 2.0\,\text{T}$): (a) The time history response plot. (b) The phase chart. (c) Poincare mapping chart.

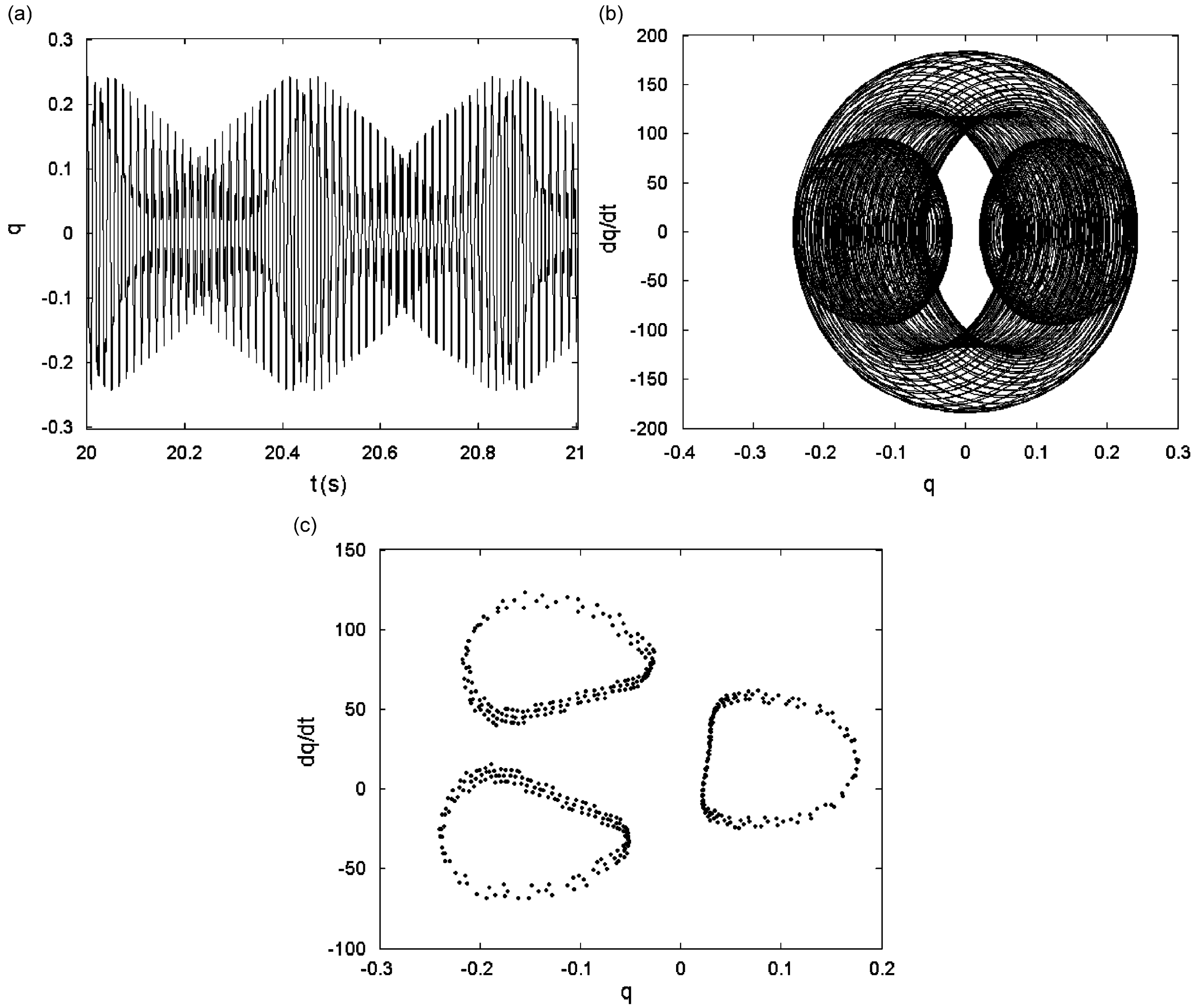

Fig. 13. The vibration characteristic plot ($B_{0z} = 0.4\,\mathrm{T}$): (a) The time history response plot. (b) The phase chart. (c) Poincare mapping chart.

motion. The phase chart is an annulus with boundary. The Poincare mapping chart still expresses three separated clusters of points set. When $B_{0z} = 0.25\,\mathrm{T}$ (Fig. 14) the points in Poincare mapping chart constitute a closed ring. The system expresses a complex quasi-period motion. From these we can know that in a certain range of parameter, with the weakening of magnetic intensity, the motion transit from stable single-frequency periodic motion to period-doubling motion and quasi-period motion.

From such results, we can see that when the subharmonic resonance happens, the system expresses a complex dynamic behavior. We can control the system vibration by choosing the proper magnetic or mechanical parameters.

5. Conclusions

(1) Magneto-elastic coupling dynamic problem is an interesting topic in recent years, and its not easy to solve these questions. This paper is about the current-conducting thin plate in electromagnetic field, and it is important theoretic meaning to study the nonlinear magneto-elasticity harmonic resonance and stability.

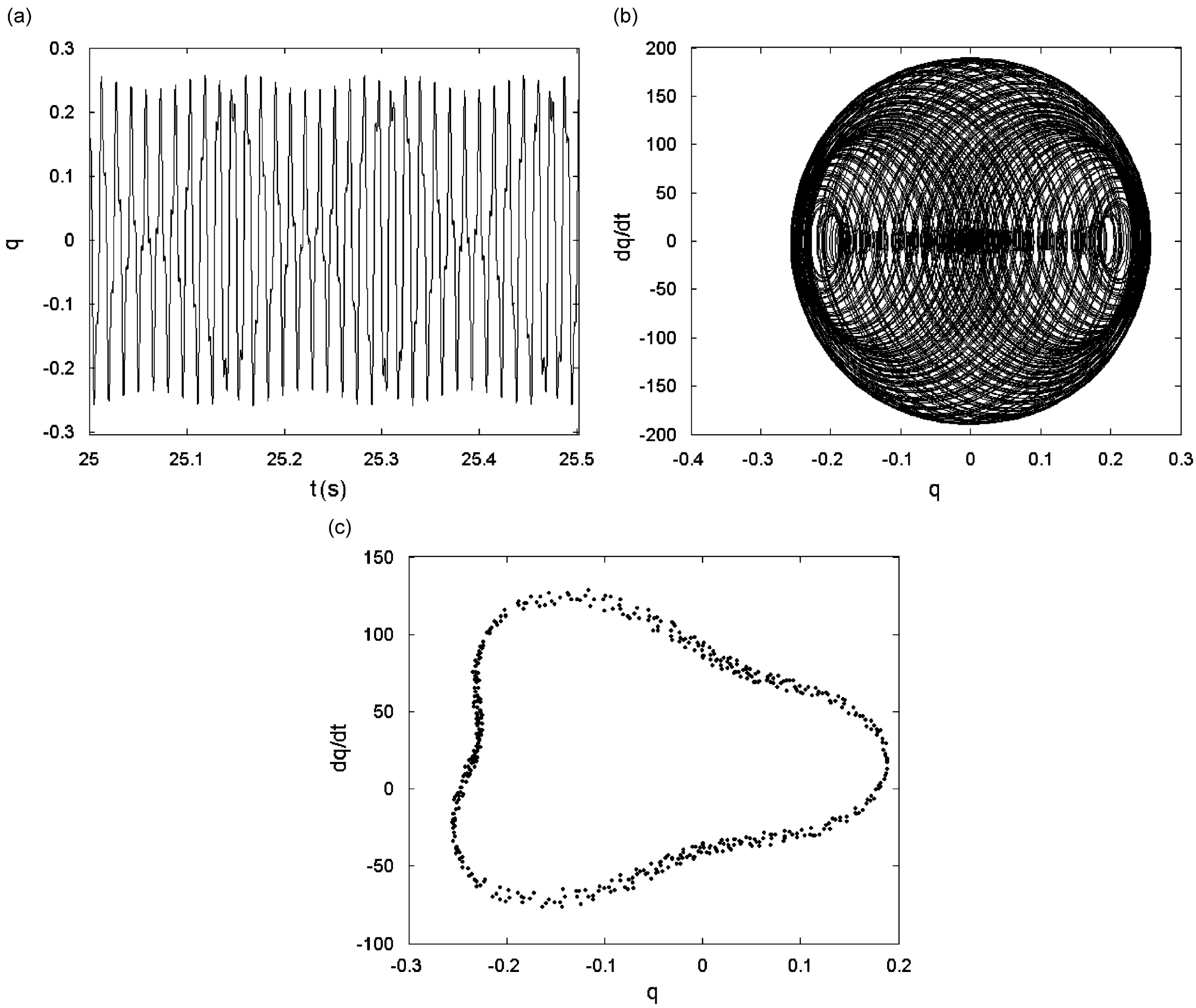

Fig. 14. The vibration characteristic plot ($B_{0z} = 0.25\,\text{T}$): (a) The time history response plot. (b) The phase chart. (c) Poincare mapping chart.

(2) Through numerical example, we analyzed existence condition, amplitude value, and dynamic phenomenon that changing with electromagnetic or mechanism, etc. These results indicate that we can control the system dynamics behavior by means of changing corresponding parameter. The results can be used as a reference to analyze the structure's complex dynamic behaviors in actual magnetic field.
(3) Based on this paper, more problems can be studied, such as, nonlinear vibration of plate in complex electromagnetic field, high dimension magneto-elastic dynamic, bifurcation and stability.

References

[1] Y.H. Pao, C.S. Yeh, A linear theory for soft ferromagnetic elastic bodies, *International Journal of Engineering Science* 11 (4) (1973) 415–436.
[2] F.C. Moon, Y.H. Pao, Vibration and dynamic instability of a beam–plate in a transverse magnetic field, *Journal of Applied Mechanics* 36 (1969) 141–149.
[3] F.C. Moon, *Magneto-Solid Mechanics*, Wiley, New York, 1984.
[4] A.C. Eringen, Theory of electric-magnetic plates, *International Journal of Engineering Science* 27 (4) (1989) 363–375.

[5] Q.S. Lu, C.W.S. To, K.L. Huang, Dynamic stability and bifurcation of an alternating load and magnetic field excited magnetoelastic beam, *Journal of Sound and Vibration* 181 (5) (1995) 873–891.
[6] W. Hai, Y. Duan, X. Pan, An analytical study for controlling unstable periodic motion in magneto-elastic chaos, *Physics Letters A* 234 (1997) 198–204.
[7] R.C.A. Thompson, T. Mullin, Routes to chaos in a magneto-elastic beam, *Chaos Solitons and Fractals* 8 (4) (1997) 681–697.
[8] G.Y. Wu, The analysis of dynamic instability on the large amplitude vibrations of a beam with transverse magnetic fields and thermal loads, *Journal of Sound and Vibration* 302 (1–2) (2007) 167–177.
[9] X.Z. Wang, J.S. Lee, X.J. Zheng, Magneto-thermo-elastic instability of ferromagnetic plates in thermal and magnetic fields, *International Journal of Solids and Structures* 40 (22) (2003) 6125–6142.
[10] S.A. Ambarcumian, G.E. Bagdasarian, M.V. Belubekian, *Magnetoelasticity of Thin Shells and Plates*, Science, Moscow, 1977.
[11] L.V. Moljchenko, *The Magnetoelasticity of Nonlinear Current-Carrying Shells*, Higher Education Press, Kiev, 1989.
[12] D.J. Hasanyan, L. Librescu, D.R. Ambur, Bucking and postbuckling of magnetoelastic flat plates carrying an electric current, *International Journal of Solids and Structures* 43 (16) (2006) 4971–4996.
[13] X.J. Zheng, J.P. Zhang, Y.H. Zhou, Dynamic stability of a cantilever conductive plate in transverse impulsive magnetic field, *International Journal of Solids and Structures* 42 (8) (2005) 2417–2430.
[14] Yuda Hu, Jiajun Qiu, Na Ta, Fundamental resonance and bifurcation of large generator end winding when its clamping plates are loose, *Applied Mathematics and Mechanics* 26 (4) (2005) 465–473.
[15] Yuda Hu, Magneto-elastic nonlinear vibration analysis of a thin conductive plate, *Engineering Mechanics* 18 (4) (2001) 89–94.
[16] Hu Yuda, Du Guojun, Li Jing, Nonlinear magnetoelastic vibration analysis of current-conducting thin plate in magnetic field, *Fifth International Conference on Nonlinear Mechanics*, Vol. 6, 2007, pp. 631–636.
[17] A.H. Nayfeh, D.T. Mook, *Nonlinear Oscillations*, Wiley, New York, 1979.
[18] Yanzhu Liu, Liqun Chen, *Nonlinear Vibration*, Higher Education Press, Beijing, 2001.